A novel 4D autonomous 2 $$\varvec{n}$$ n -butterfly wing chaotic attractor

Fadhil Rahma Tahir, Ramzy S. Ali, Viet-Thanh Pham, Arturo Buscarino, Mattia Frasca, et al.

Nonlinear Dynamics
An International Journal of Nonlinear Dynamics and Chaos in Engineering Systems

ISSN 0924-090X

Nonlinear Dyn
DOI 10.1007/s11071-016-2853-7

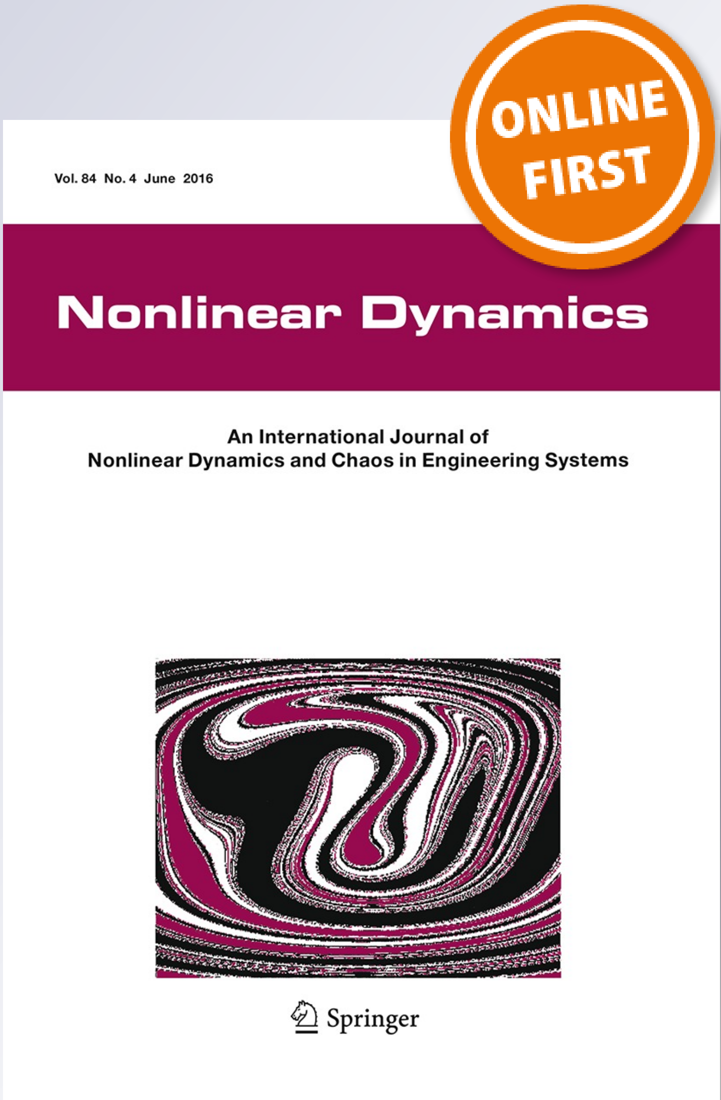

Springer

Nonlinear Dyn
DOI 10.1007/s11071-016-2853-7

ORIGINAL PAPER

A novel 4D autonomous 2n-butterfly wing chaotic attractor

Fadhil Rahma Tahir · Ramzy S. Ali · Viet-Thanh Pham · Arturo Buscarino · Mattia Frasca · Luigi Fortuna

Received: 16 February 2016 / Accepted: 13 May 2016

Abstract This paper presents a four-dimensional (4D) autonomous chaotic system. The new system is obtained by introducing the state feedback and a novel n-well potential function to the third-order Duffing system. The proposed potential function enables us to create butterfly wing chaotic attractors. The new system can generate n-scroll and 2n-butterfly wing chaotic attractors. The basic dynamical behaviors and properties of this system are investigated, such as equilibriums, stability of equilibrium points, attractors, and Lyapunov exponents. The circuit realization and experimental results are also presented.

Keywords Chaos · Butterfly wing attractor · Autonomous Duffing system · Circuit

1 Introduction

Recently, there has been increasing interest in the design and implementation of chaotic systems. It has been found that chaos has a theoretical and practical importance in many fields such as engineering, medicine, secure communications, and so on [1–6]. This has motivated an intense research that has led to the discovery of many chaotic systems [7–10].

In particular, the theoretical design and circuit implementation of various complex multiscroll chaotic systems has been a central subject of the real-world applications of various chaos-based technologies and information systems [11–13]. For example, by using a 2D chaotic sequence achieved from multi-scroll chaotic attractors fingerprint images were encrypted [14]. By considering the synchronization of Chua's circuits with multi-scroll attractor, Gamez-Guzman et al. [15] transmitted encrypted audio and image information successfully. Another example of application is the work by Yalcin [16] who improved the entropy of a random number generator by increasing the number of scrolls in a generalized Jerk circuit. As a result, approaches to generate multiscroll

F. R. Tahir · R. S. Ali
Department of Electrical Engineering, College of Engineering, University of Basrah, Basrah, Iraq
e-mail: fadhilrahma.creative@gmail.com

R. S. Ali
e-mail: ramzy.salim@uobasrah.edu.iq

V.-T. Pham (✉)
School of Electronics and Telecommunications, Hanoi University of Science and Technology, 01 Dai Co Viet, Hanoi, Vietnam
e-mail: pvt3010@gmail.com

A. Buscarino · M. Frasca · L. Fortuna
Dipartimento di Ingegneria Elettrica Elettronica e Informatica, Università degli Studi di Catania, Viale A. Doria 6, 95125 Catania, Italy
e-mail: arturo.buscarino@dieei.unict.it

M. Frasca
e-mail: mattia.frasca@dieei.unict.it

L. Fortuna
e-mail: lfortuna@diees.unict.it

Published online: 27 May 2016

chaotic attractors have been studied in many researches [11,17,18]. In addition, multiple-wing chaotic attractors can be constructed based on known chaotic systems [19–26]. Multiple-wing chaotic system has also been used in chaos-based applications [27]. Finding new chaotic systems which can generate both multi-scroll and multiple-wing chaotic attractors is, despite its potential interest, a topic not yet fully explored in the literature.

The aim of this paper is to introduce a novel chaotic system originating from the Duffing equations which can generate n-scroll and $2n$-butterfly wing chaotic attractors. The rest of the paper is organized as follows. The design of the new 4D Duffing system-based chaotic attractor is described in Sect. 2. The basic properties of the chaotic system are investigated numerically in Sect. 3. A modular circuit is proposed for realizing various multi-butterfly wing chaotic attractors in Sect. 4. Conclusions are given in Sect. 5.

2 Model of the new 4D chaotic Duffing system

In Ref. [28], a dynamical model of an autonomous three-dimensional Duffing system described by the following equations

$$\begin{cases} \dot{x} = y \\ \dot{y} = x - x^3 + \mathrm{d}y - \beta z \\ \dot{z} = r\,(y - z)\,, \end{cases} \tag{1}$$

is reported. Here x, y, z are three independent dynamical variables, while d , r and β are constant parameters. The system is chaotic for a suitable choice of the parameters as detailed in [28].

Based on system (1), the new chaotic system is generated by replacing the cubic nonlinearity in Eq. (1) by a nonlinear function $h(x)$ and introducing a state feedback controller w to the second equation as follows

$$\begin{cases} \dot{x} = y \\ \dot{y} = h\,(x) + \mathrm{d}y - \beta z + bw \\ \dot{z} = r\,(y - z) \\ \dot{w} = -cxy - mw, \end{cases} \tag{2}$$

where d, β, b, r, c and m are the parameters of the system. We adopt two different definitions for the nonlinear function $h(x)$:

(i) To generate a $2n$-butterfly wing chaotic attractor in the $y-w$ plane and a chaotic attractor with an even number of scrolls in the $x-y$ plane, the nonlinear function $h(x)$ is fixed as

$$h\,(x) = -x + a \sum_{k=-(N-1)}^{N-1} \tanh\left(ax + \mathrm{sgn}\,(k)\, a^{|k|+2}\right) \tag{3}$$

where $a = 2$ and $N \geq 1$. In this case, the number of wings in the $y-w$ plane is $2n$ with $n = 2N$, while the number of scroll in the $x-y$ plane is n.

(ii) To obtain a $2n$-butterfly wing chaotic attractor in the $y-w$ plane and a chaotic attractor with an odd number of scrolls in the $x-y$ plane, the nonlinear function $h(x)$ is selected as:

$$h\,(x) = -\,(x + a) + a \sum_{k=-(N-2)}^{N-1} \tanh\left(ax + \mathrm{sgn}\,(k)\, a^{|k|+2}\right) \tag{4}$$

where $a = 2$ and $N \geq 2$. In this case, the number of wings in the $y-w$ plane is $2n$ with $n = 2N-1$, while the number of scroll in the $x-y$ plane is n.

Our numerical simulations show that the new system (2) for selected values of the parameters displays sophisticated chaotic dynamical behaviors. The phase portraits of the new system (2) are shown in Figs. 1 and 2, for an illustrative set of parameters: $N = 1$, $d = 0.35$, $b = 0.125$, $\beta = 1.95$, $r = 0.45$, $c = 0.45$, $m = 15$. The attractor is a two-scroll chaotic attractor on the $x-y$ plane (Fig. 1a). Interestingly, the attractor is a four-wing chaotic attractor as it appears clearly from the projection on the $y-w$ plane (Fig. 2). In addition, selecting $N > 1$, a new $2n$-butterfly wing attractor, for example with $n = 3$, or $n = 6$, can be obtained as illustrated in Fig. 3.

3 Dynamical properties of the new chaotic system

In this Section, some basic properties and complex dynamics of system (2) are illustrated, including dissipativity, equilibrium points and Lyapunov exponents.

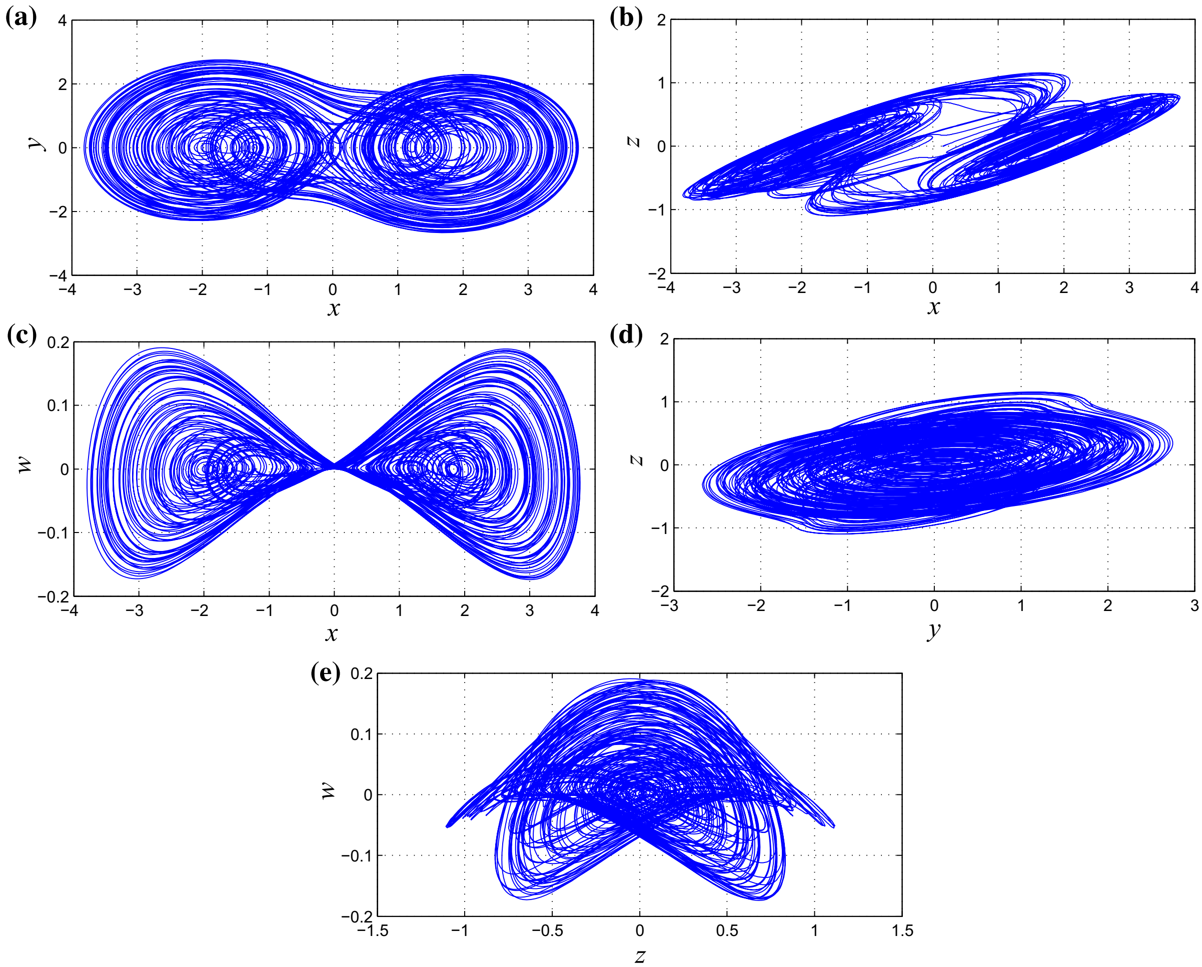

Fig. 1 Phase portrait of 4D chaotic system (2) for $N = 1$, $d = 0.35$, $b = 0.125$, $\beta = 1.95$, $r = 0.45$, $c = 0.45$, $m = 15$ in: **a** $x - y$ plane, **b** $x - z$ plane, **c** $x - w$ plane, **d** $y - z$ plane, and **e** $z - w$ plane

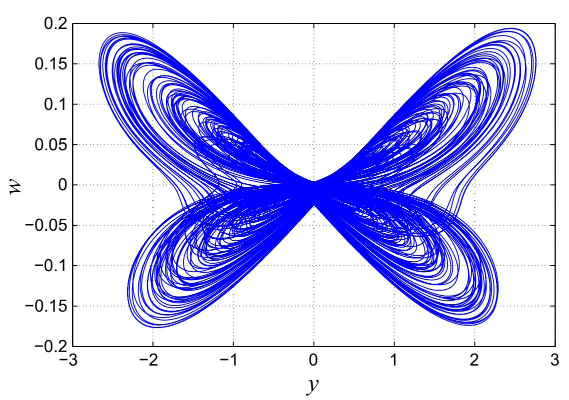

Fig. 2 Chaotic 4-butterfly wing attractor in $y - w$ plane. The parameters are selected as in Fig. 1

3.1 Dissipativity

From system (2), one has

$$\nabla V = \frac{\partial \dot{x}}{\partial x} + \frac{\partial \dot{y}}{\partial y} + \frac{\partial \dot{z}}{\partial z} + \frac{\partial \dot{w}}{\partial w} = -\left(-d + r + m\right). \tag{5}$$

For the chaotic system to become dissipative, it is required that $(-d + r + m) > 0$. That is, a volume element V_0 is contracted by the flow into a volume element $V_0 e^{-(-d+m+r)t}$ in time t. This means that each volume containing the trajectory of dynamical system (2) shrinks to zero as $t \rightarrow \infty$ at exponential rate

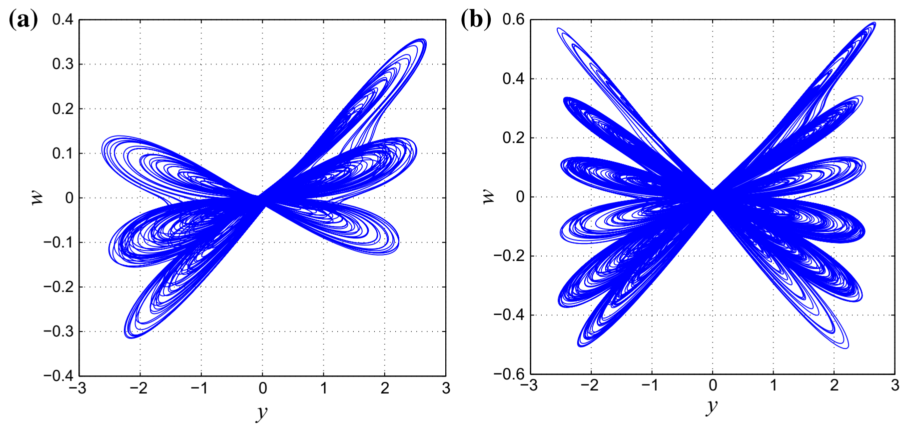

Fig. 3 Chaotic $2n$-butterfly wing attractors: **a** 6-butterfly wing ($N = 2$, $n = 3$), **b** 12-butterfly wing ($N = 3$, $n = 6$)

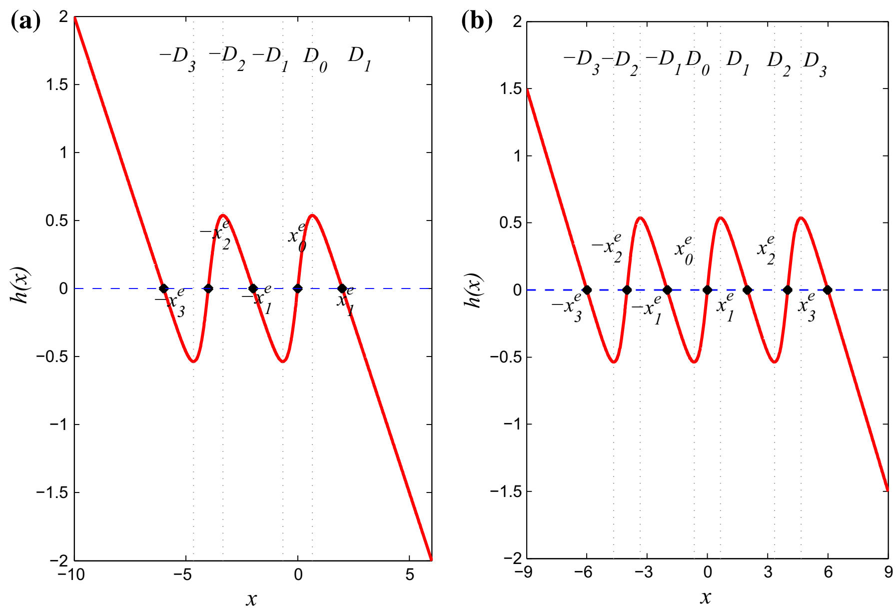

Fig. 4 The nonlinear function $h(x)$ and its characteristic regions when generating: **a** 6-wing attractor; **b** 8-wing attractor

$(-d + r + m)$. Numerical simulations confirm that, when condition (5) is satisfied, system trajectories are ultimately confined to an attractor.

3.2 Equilibrium and stability

The equilibrium points of system (2) can be easily found by solving the following set of equations:

$$\begin{cases} y = 0 \\ h(x) + dy - \beta z + bw = 0 \\ r(y - z) = 0 \\ -cxy - mw = 0. \end{cases} \tag{6}$$

The equilibrium points $\pm x_k^e$ $(k = 0, 1, 2, \ldots, N)$ are located at the intersection of the nonlinear function $h(x)$ and the x-axis in the state space. Therefore, the set of equilibrium points is given by

$$E = \{(x; 0; 0; 0)| \\ x = -x_N^e, -x_{N-1}^e, \ldots, -x_1^e, x_0^e, x_1^e, \ldots, x_{N-1}^e\} \tag{7}$$

For instance, Fig. 4a, b show the nonlinear functions $h(x)$ that correspond to chaotic attractors with 6 wings (3 scrolls) and 8 wings (4 scrolls), respectively. In Fig. 4a, b, the value of N has been fixed as $N = 2$. For this choice of N, system (2) has five and seven equilibrium points, respectively. Here the characteristic regions are denoted by $\pm D_k$.

It is worth to note that the equilibrium points are located on the x-axis. Its stability is determined by the eigenvalues of the Jacobian matrix at equilibrium points $E(\pm x_k^e, 0, 0, 0)$ $(k = 0, 1, 2, \ldots, N)$ given by

$$J(E) = \begin{bmatrix} 0 & 1 & 0 & 0 \\ \frac{\partial h_i(x)}{\partial x}\Big|_{x=\pm x_k^e} & d & -\beta & b \\ 0 & r & -r & 0 \\ -cy|_{y=0} & -cx|_{x=\pm x_k^e} & 0 & -m \end{bmatrix}. \quad (8)$$

For $N = 1$ and the parameters fixed as $d = 0.35$, $b = 0.125$, $\beta = 1.95$, $r = 0.45$, $c = 0.45$, $m = 15$, then the Jacobian matrix around the zero equilibrium point $E(0, 0, 0, 0)$ has four eigenvalues: $\lambda_1 = 1.7036$, $\lambda_2 = -1.0458$, $\lambda_3 = -0.7578$, $\lambda_4 = -15$ which implies that the zero equilibrium is unstable. For the equilibrium points $E(\pm 2, 0, 0, 0)$, the eigenvalues are $\lambda_{1,2} = 0.0738 \pm j1.3233$, $\lambda_3 = -0.2549$, $\lambda_4 = -14.9927$ and $\lambda_{1,2} = 0.0813 \pm j1.3211$, $\lambda_3 = -0.2554$, $\lambda_4 = -15.0073$, which implies that the equilibrium points are saddle with index 2 which generate the scrolls. Similarly, for the other cases, we can use the Jacobian matrix to study the stability of the equilibriums with respect to selected parameters [29].

3.3 Lyapunov exponents

Lyapunov exponents measure the exponential rates of the divergence and convergence of nearby trajectories in phase space of chaotic system [30]. As well known, a system is chaotic when it has at least one positive Lyapunov exponent. For convenience, we may order the Lyapunov exponents in decreasing order. For the parameters of Fig. 1, we obtain Lyapunov exponents as $\lambda_1 = 0.1032$, $\lambda_2 = 0$, $\lambda_3 = -0.2004$, $\lambda_4 = -15.0003$, respectively, which demonstrated that the system shown in Fig. 1 is chaotic. The possibility of generating hyperchaotic attractors of new system (2) has been also investigated by exploring the parameter space. However, hyperchaos has not been observed in such 4D system with multiple-wing attractors.

Lyapunov exponents have been studied with respect to the many parameters appearing in the system. We have found large windows of chaotic behavior. In Fig. 5, we report, for instance, the Lyapunov exponents of system (2) when the parameter d is varied. Figure 5 shows the onset of chaos for $d > 0.32$.

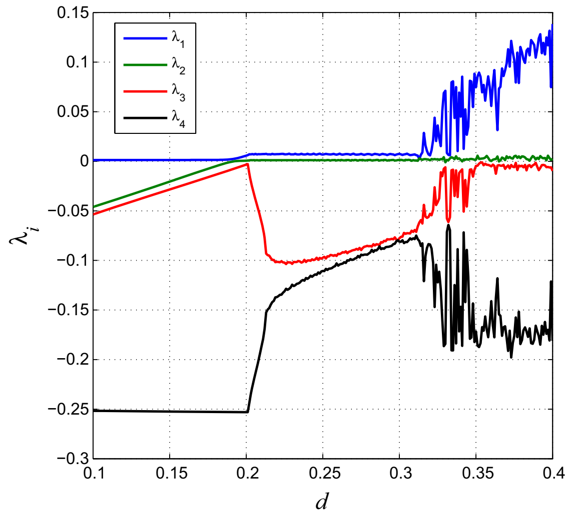

Fig. 5 Lyapunov exponents of system (2) with respect to d for $N = 1$, $b = 0.125$, $\beta = 1.95$, $r = 0.45$, $c = 0.45$, $m = 15$

4 Circuit implementation and experimental results

In this Section, the circuit implementation of the mathematical model (2) is discussed. The circuit is based on operational amplifiers, so that a rescaling is needed to met the dynamical range of these devices. For this reason, the state variable x of system (2) has been rescaled down and the whole system rewritten as:

$$\begin{cases} \dot{X} = 0.5Y \\ \dot{Y} = h_i(2X) + \mathrm{d}Y - \beta Z + bW \\ \dot{Z} = rY - rZ \\ \dot{W} = -2cXY - mW, \end{cases} \quad (9)$$

where $X = \frac{x}{2}$, $Y = y$, $Z = z$, and $W = w$. The electronic circuit to realize (9) is presented in Fig. 6 and is governed by the following circuit equations

$$\begin{cases} \frac{\mathrm{d}v_{C_1}}{\mathrm{d}t} = \frac{1}{R_1C_1} v_{C_2} \\ \frac{\mathrm{d}v_{C_2}}{\mathrm{d}t} = \frac{1}{R_2C_2} h\left(2v_{C_1}\right) + \frac{1}{R_3C_2} v_{C_2} \\ \qquad -\frac{1}{R_4C_2} v_{C_3} + \frac{1}{R_5C_2} v_{C_4} \\ \frac{\mathrm{d}v_{C_3}}{\mathrm{d}t} = \frac{1}{R_6C_3} v_{C_2} - \frac{1}{R_7C_3} v_{C_3} \\ \frac{\mathrm{d}v_{C_4}}{\mathrm{d}t} = -\frac{1}{10R_8C_4} v_{C_1} v_{C_2} - \frac{1}{R_9C_4} v_{C_4}, \end{cases} \quad (10)$$

where v_{C_1}, v_{C_2}, v_{C_3} and v_{C_4} are voltages across the capacitors C_1, C_2, C_3 and C_4. Therefore, the state vari-

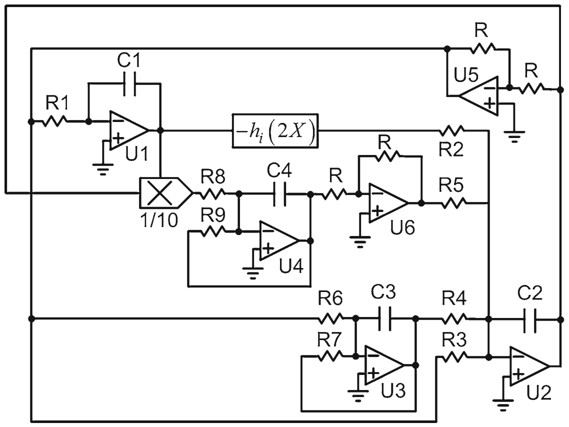

Fig. 6 Circuit diagram implementing the new chaotic system (9)

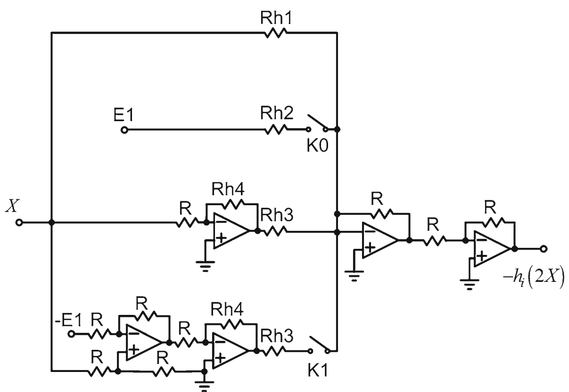

Fig. 7 Electrical scheme of the circuit realizing the nonlinearity $-h_i(2X)$

ables in Eq. (9), i.e., X, Y, Z, W are implemented as the voltages across corresponding capacitors.

The circuit only consists of common off-the-shelf discrete components such as resistors, capacitors, operational amplifiers and a multiplier (AD633). The power supplies are fixed to $\pm 15V_{\mathrm{DC}}$, and TL084 operational amplifiers are used. Eq. (10) match Eq. (2) with $d = \frac{R}{R_3}$, $b = \frac{R}{R_5}$, $\beta = \frac{R}{R_4}$, $r = \frac{R}{R_6}$, $c = \frac{R}{20R_8}$, and $m = \frac{R}{R_9}$ where $R = R_2$. The nonlinear function $-h_i(2X)$ in Fig. 6 is implemented by the circuitry of Fig. 7. The nonlinearity is designed in a modular way so that it can be changed by choosing the on–off switches. By adapting the nonlinearity, the circuit on Fig. 6 can generate various $2n$-butterfly wing attractors. Table 1 summarizes the states of switches and the number of wings in the attractors. As an example, we have considered a 6-wing chaotic attractor, obtained by using the circuit of Fig. 6 with the switches set as S1 in ON state. In

Table 1 On–off switches, and the number of butterfly swings (in v_{C_2}–v_{C_4} plane) of the designed circuit

K_0	K_1	Butterfly wings
Off	Off	4
On	On	6

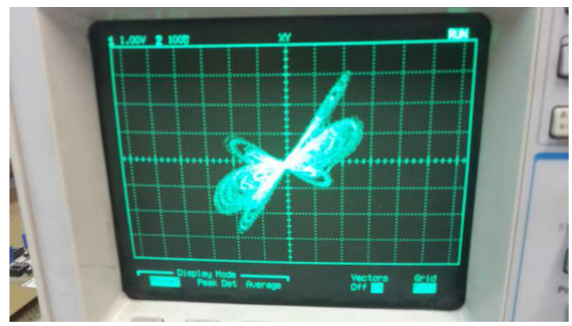

Fig. 8 Experimental results: projection on the $Y - W$ plane of the attractor obtained by the circuit of Fig. 6. *Horizontal axis* 1 V/div. *Vertical axis* 100 mV/div

this case, the output of the circuit in Fig. 7 is written as

$$\begin{aligned} h_i(2X) = &-\frac{R}{R_{h1}}X - \frac{R}{R_{h2}}E_1 \\ &+\frac{R}{R_{h3}}V_{\mathrm{sat}}\tanh\left(\frac{R_{h4}}{R}\frac{X}{V_{\mathrm{sat}}}\right) \\ &+\frac{R}{R_{h3}}V_{\mathrm{sat}}\tanh\left(\frac{R_{h4}}{R}\frac{X+E_1}{V_{\mathrm{sat}}}\right), \end{aligned} \tag{11}$$

where V_{sat} is the saturation voltage of the operational amplifier. Eq. (11) match Eq. (4) with $a = \frac{R}{R_{h2}}\frac{E_1}{1V_{\mathrm{DC}}} = \frac{R}{R_{h3}}\frac{V_{\mathrm{sat}}}{1V_{\mathrm{DC}}} = \frac{R_{h4}}{2R}\frac{1V_{\mathrm{DC}}}{V_{\mathrm{sat}}}$. We choose the components in the circuit to realize the reported parameter values. Therefore, the value of components is selected as follows $R_1 = 20\,\mathrm{k\Omega}$, $R_2 = R = 10\,\mathrm{k\Omega}$, $R_3 = 28.57\,\mathrm{k\Omega}$, $R_4 = 5.128\,\mathrm{k\Omega}$, $R_5 = 80\,\mathrm{k\Omega}$, $R_6 = R_7 = 22.22\,\mathrm{k\Omega}$, $R_8 = 1.111\,\mathrm{k\Omega}$, $R_9 = 0.666\,\mathrm{k\Omega}$, $C_1 = C_2 = C_3 = C_4 = 10nF$, $R_{h1} = 5\,\mathrm{k\Omega}$, $R_{h2} = R = 10\,\mathrm{k\Omega}$, $R_{h3} = 71.25\,\mathrm{k\Omega}$, $R_{h4} = 570\,\mathrm{k\Omega}$, and $E_1 = 2V_{\mathrm{DC}}$. The experimental attractor, corresponding to this set of parameters, as observed on the oscilloscope (projection on the $Y - W$ plane), is reported in Fig. 8.

5 Conclusion

In this paper, we have presented a novel fourth-order chaotic system and its complex dynamics. Interestingly, the system has been constructed with the introduction of a new potential function that is suitable for the purpose of generating n-scroll and 2n-butterfly wing chaotic attractors. Such new potential function can be implemented easily because its basic block is the hyperbolic tangent function that corresponds to operational amplifier saturation [31–33]. The electronic circuitry of the new chaotic system has been designed and realized by physical components. We have found a good agreement between simulations and experiments. Such new chaotic system can be used in chaos-based engineering applications due to its capability of producing multiscroll chaotic signals with a quite simple circuitry.

References

1. Buscarino, A., Fortuna, L., Frasca, M., Muscato, G.: Chaos does help motion control. Int. J. Bifurc. Chaos **17**, 3577–3581 (2007)
2. Chen, G., Yu, X.: Chaos Control: Theory and Applications. Springer, Berlin (2003)
3. Chua, K., Zheng, W.: Chaos in Electric Drive Systems Analysis. Control and Applications. Wiley, Berlin (2011)
4. Khan, M., Shah, T., Gondal, M.A.: An efficient technique for the construction of substitution box with chaotic partial differential equation. Nonlinear Dyn. **73**, 1795–1801 (2013)
5. Tang, W., Zhang, J.: A novel bounded 4D chaotic system. Nonlinear Dyn. **67**, 2455–2465 (2012)
6. Fortuna, L., Frasca, M., Rizzo, A.: Chaotic pulse position modulation to improve the efficiency of sonar sensors. IEEE Trans. Instrum. Meas. **52**, 1814–1890 (2003)
7. Lorenz, E.N.: Deterministic nonperiodic flow. J. Atmos. Sci. **20**, 130–141 (1963)
8. Chen, G., Ueta, T.: Yet another chaotic attractor. Int. J. Bifurc. Chaos **9**, 1465–1466 (1999)
9. Lü, J., Chen, G.: A new chaotic attractor coined. Int. J. Bifurc. Chaos **12**, 659–661 (2002)
10. Lü, J., Chen, G., Chen, D., Celikovsky, S.: Bridge the gap between the Lorenz system and the Chen system. Int. J. Bifurc. Chaos **12**, 2917–2926 (2002)
11. Lü, J., Chen, G.: Generating multiscroll chaotic attractors: theories, methods and applications. Int. J. Bifurc. Chaos **16**, 775–858 (2006)
12. Ma, J., Wu, X.Y., Qin, H.X.: Realization of synchronization between hyperchaotic systems by using a scheme of intermittent linear coupling. Acta Phys. Sin. **62**, 170502 (2013)
13. Ma, J., Wu, X., Chu, R., Zhang, L.: Selection of multi-scroll attractors in jerk circuits and their verification using Pspice. Nonlinear Dyn. **76**, 1951–1962 (2014)
14. Han, F., Hu, J., Yu, X., Wang, Y.: Fingerprint images encryption via multi-scroll chaotic attractors. Appl. Math. Comput. **185**, 931–939 (2007)
15. Gamez-Guzman, L., Cruz-Hernandez, C., Lopez-Gutierrez, R., Garcia-Guerrero, E.E.: Synchronization of Chua's circuits with multi-scroll attractors: application to communication. Commun. Nonlinear Sci. Numer. Simul. **14**, 2765–2775 (2009)
16. Yalcin, M.E.: Increasing the entropy of a random number generator using n-scroll chaotic attractors. Int. J. Bifurc. Chaos **17**, 4471–4479 (2007)
17. Zidan, M.A., Radwan, A.G., Salama, K.N.: Controllable V-shape multiscroll butterfly attractors system and circuit implementation. Int. J. Bifurc. Chaos **22**, 1250142 (2012)
18. Wang, L.: 3-scroll and 4-scroll chaotic attractors generated form a new 3-D quadratic autonomous system. Nonlinear Dyn. **56**, 453–462 (2009)
19. Elwakil, A.S., Özoguz, S., Kennedy, M.P.: Creation of a complex butterfly attractor using a novel Lorenz-type system. IEEE Trans. Circuit Syst. I **49**, 527–530 (2002)
20. Elwakil, A.S., Özoguz, S., Kennedy, M.P.: A four-wing butterfly attractor from a fully autonomous system. Int. J. Bifurc. Chaos **13**, 3093–3098 (2003)
21. Dadras, S., Momeni, H.R., Qi, G.: Analysis of a 3D smooth autonomous system with different wing chaotic attractors and transient chaos. Nonlinear Dyn. **62**, 391–405 (2010)
22. Wang, Z., Qi, G., Sun, Y., Wyk, B.J., Wyk, M.A.: A new type of four-wing chaotic attractors in a 3-D quadratic autonomous system. Nonlinear Dyn. **60**, 443–457 (2010)
23. Yu, S., Tang, W.K.S., Lu, J., Chen, G.: Design and implementation of multi-wing butterfly chaotic attractors via Lorenz-type system. Int. J. Bifurc. Chaos **20**, 29–41 (2010)
24. Yu, S., Lü, J., Chen, G., Yu, X.: Generating grid multi-wing chaotic attractors by constructing heteroclinic loops into switching systems. IEEE Trans. Circuits Syst. I Exp. Briefs **58**, 314–318 (2011)
25. Lai, Q., Guan, Z.H., Wu, Y., Liu, F., Zhang, D.X.: Generation of multi-wing chaotic attractors from a Lorenz-like system. Int. J. Bifurc. Chaos **23**, 1350152 (2013)
26. Yun, H.: A family of multi-wing chaotic attractors and its circuit implementation. Acta Phys. Sin. **63**, 080505 (2014)
27. Liu, G., Yang, W., Liu, W., Dai, Y.: Designing S-boxes based on 3-D four-wing autonomous chaotic system. Nonlinear Dyn. **82**, 1867–1877 (2015)
28. Tamasevicius, A., Bumeliene, S., Kirvaitis, R., Mykolaitis, G., Tamaseviciute, E., Lindberg, E.: Autonomous Duffing–Holmes type chaotic oscillator. Electron. Elect. Eng. J. **93**, 43–46 (2009)
29. Yu, S., Lü, J., Chen, G.: A family of n-scroll hyperchaotic attractors and their realization. Phys. Lett. A **364**, 244–251 (2007)
30. Wolf, A., Swift, J.B., Swinney, H.L., Vastano, J.A.: Determining Lyapunov exponents from a time series. Phys. D **16**, 285–317 (1985)
31. Sedra, A.S., Smith, K.C.: Microelectronic Circuits. Oxford University Press, Oxford (2003)
32. Buscarino, A., Fortuna, L., Frasca, M., Sciuto, G.: Design of time-delay chaotic electronic circuits. IEEE Trans. Circuits Syst. I Regul. Pap. **58**, 1888–1896 (2011)
33. Banerjee, T., Biswas, D., Sarkar, B.C.: Design and analysis of a first order time-delayed chaotic system. Nonlinear Dyn. **70**, 721–734 (2012)